Microchimica Acta (2018) 185: 60
https://doi.org/10.1007/s00604-017-2600-x

ORIGINAL PAPER

Hemoglobin-incorporated iron quantum clusters as a novel fluorometric and colorimetric probe for sensing and cellular imaging of Zn(II) and cysteine

Naimeh Hashemi[1] · Zahra Vaezi[1] · Mosslim Sedghi[1] · Hossein Naderi-Manesh[1]

Received: 7 September 2017 / Accepted: 1 December 2017 / Published online: 18 December 2017

Abstract

The authors describe a novel water-soluble, stable, biocompatible, and highly fluorescent probe consisting of iron quantum clusters incorporated into human adult hemoglobin (Hb-FeQCs). The Hb-FeQCs were characterized by various spectroscopic techniques. The probe displays strong absorption and yellow fluorescence with a peak centered at 567 nm (photo-excited at 460 nm). The Hb-FeQCs show excellent photostability over a wide range of pH values (5–12), even in the presence of high electrolyte concentrations. A colorimetric and a fluorometric method were worked out for the quantitation Zn(II) and cysteine in aqueous solution. Zinc ions induce a visible color change from brown to yellow. The sensitivity of Hb-FeQCs towards other metal ions was negligible, with the exception of Co^{2+} and Cu^{2+}, which caused a modest interference. The Hb-FeQCs were exploited in a sensitive and selective turn-on fluorescence assay for Zn^{2+}. It is also found that cysteine quenches the fluorescence of the Hb-FeQCs/Zn(II) complex. Under the optimized conditions, the probe has a linear response in the 0.04 to 2.2 μM Zn(II) concentration range, with a 48 nM detection limit. Response to cysteine is linear in the 1–60 μM concentration range, with a 0.25 μM limit of detection. This fluorescent probe undergoes fluorescent emission intensity enhancement upon binding to zinc ions in living normal human fibroblast cells under visible lamp. The cellular imaging capability and very low cytotoxicity of this soluble iron quantum clusters can be potentially extended as an exciting sub-nanoplatform with promising biomaterial applications.

Keywords Fluorescent nanocluster · Hemoglobin · Iron Quantum clusters · Chemiluminescence · On-off fluorescence switch · Colorimetric probe · Zinc(II) detection · Cysteine · Cell imaging · Cytotoxicity

Highlights
- Novel water-soluble iron quantum clusters in protein (Hb-FeQCs) exhibit yellow emission.
- Zinc ions induce a visible color change of Hb-FeQCs solution.
- Hb-FeQCs/Zn(II) complex is a highly selective fluorescence "turn-off" probe for cysteine.
- Nontoxic Hb-FeQCs detect Zn^{2+} in living cells with nanomolar levels under visible light.

Electronic supplementary material The online version of this article (https://doi.org/10.1007/s00604-017-2600-x) contains supplementary material, which is available to authorized users.

✉ Hossein Naderi-Manesh
naderman@modares.ac.ir

[1] Department of Nanobiotechnology/Biophysics, Faculty of Biological Science, Tarbiat Modares University, Tehran 14115-154, Iran

Introduction

Among the synthesized nanomaterials in the recent past, metal nanoclusters (MNCs) or quantum clusters (QCs) have become more prominent among the synthesized nanomaterial, due to their novel optical, electronical and chemical properties. They are significantly different from nanoparticles (NPs) that show plasmon absorption [1]. These unique properties make them attractive for various kinds of applications such as metal ion sensing [2, 3], catalysis [4], and bio-imaging [5]. In current researches, noble metals QCs such as Au, Ag, Cu, Ni, and Cd have been well studied, but, better biocompatible, cheaper, unique catalytic and magnetic properties of Fe make Fe-QCs important candidates. To date, a few experimental studies have given direct insight into iron nanoclusters [6], primarily

due to the difficulty in preparing highly stable and extremely tiny Fe particles. Additionally, sub nanometre-sized Fe^0 intrinsically suffers from instability because of easy surface oxidation on exposure to air and in the presence of water. Therefore, it would be of great interest to develop very stable, highly luminescent, biocompatible iron quantum clusters (FeQCs) with excitation and emission in the visible range. The fluorescence of QCs correlates not only with the metal quantization effect but also with the surface ligands or scaffolds. The use of hemoglobin (Hb) as an iron-containing protein, as well as a protective agent in the synthesis of QCs provides many advantages, such as excellent stability, low toxicity, good water solubility, high photoluminescence quantum yield, and biocompatibility [5–7]. Monitoring the sub-cellular region using fluorescence imaging technique with non-toxic QCs and detection of biologically significant metal ions in nanomolar concentration is an important in clinical technology [8, 9].

Although zinc ion plays a prominent role in regulating many biological processes including regulation of gene expression and cellular apoptosis, its intensified level in body induces toxicity and cause deleterious effects on vital biological organs such as liver and kidneys, disturbance of copper metabolism, and reduced iron function [10]. The "free zinc" in certain cells is associated to some serious neurological diseases such as Alzheimer's, Parkinson's disease [11], certain forms of cancers, and even possesses a strong affinity towards the cysteine-rich regions of the prion protein (PrP) causing misfolding and protein fibrilization [12].

Since conventional atomic and molecular spectroscopic techniques for the detection of Zn^{2+} ions require expensive instruments and/or complicated sample preparation processes, detection with nano-biosensors, which the ability to prevent the interference of some heavy and transition metal ions such as Co^{2+}, Ni^{2+}, Cu^{2+}, Cd^{2+}, and Hg^{2+}, presents the potential for simple, low-cost, and facile tracking of Zn^{2+} ions in biological, toxicological and environmental samples [13, 14]. On the other hand, amino acids which are generally weak chromophores in their native form are a challenging subject for monitoring individually in biological samples. Cysteine (Cys), one of the most important small biothiols, is involved in multiples of vital cells process, such as the building block in protein synthesis, bio-catalysis, detoxification, and metabolism in live organisms [2]. More attempts to introduce new sensing methods for sensitive and selective determination of Cys in biological fluids has become more necessary and attracted great interest. Many strategies have been reported for turn-on and ratio metric Zn(II) sensors [8, 13–15], However, to the best of our knowledge, it has not been addressed in any previous report the detection of zinc ion via Hb-FeQCs. Here, we report a colorimetric assay for the direct detection of Zn^{2+} and Cys by accomplishing a novel fluorescent switching sensor. These assays are allowed ultrasensitive fluorescence response and selective detection of them based on Hb protected FeQCs. A schematic presentation of the "on-off" behavior of the synthesized Hb-FeQCs is shown in Scheme 1.

In vitro cell viability studies carried out with Human Foreskin Fibroblasts (HFF) cells confirmed the non-cytotoxic nature of the Hb-stabilized FeQCs and their suitability for biological applications. Most notably, Hb-FeQCs shows good cell membrane permeability and can be successfully applied to the imaging of Zn^{2+} and Cys in living cells.

Experimental

Materials

Analytical-grade chemical reagents were used without further purification. Hemoglobin and $NaBH_4$ were obtained from Sigma-Aldrich. All metal salts, amino acids, and Piperidine were purchased from Merck. Fetal bovine serum (FBS) and Dulbecco's Modified Eagle's Medium (DMEM) were obtained from Gibco, and 7-Hydroxy-3H-phenoxazin-3-one-10-oxide (Alamar blue assay) from Sigma-Aldrich. Doubly distilled deionized water was produced using a Millipore-Q water system and used in all experiments.

Apparatus

All fluorescence measurements were monitored using a Perkin Elmer LS-55 fluorescence spectrometer with a xenon lamp as a source of excitation and UV–vis spectroscopy was performed by a Perkin Elmer Lambda 25 UV-Visible spectrometer (Perkin-Elmer, UK, www.perkinelmer.com). Particle size analysis and zeta potential measurement of FeQCs were determined using Zetasizer Nano ZS95 (Malvern Instruments Ltd., UK, www.malvern.com) with a wavelength of 663 nm red laser at 25 °C. Fourier transform infrared spectroscopy (FTIR) was carried out with a Bruker Tensor 27 Spectrometer (Bruker, Japan, www.bruker.co.jp) using deride Hb-FeQCs samples and KBr pellets in the range of 4000 to 400 cm^{-1}, at room temperature. CD spectra were measured with a Jasco J-715 CD spectrometer (JASCO, Japan, www.jasco.co.jp) at ambient temperature using a quartz cuvette with a 5 mm path length from 700 to 190 nm at a scan rate of 20 nm. The data were smoothed using the Jasco J-715 software, which includes a fast Fourier-transform noise reduction routine. The results were expressed in term of the ellipticity [θ] (degree cm^2 $dmol^{-1}$). Magnetic measurements were performed in a TDK VSM with an electromagnet that can produce field up to 1.5 T.

Fluorescence measurements

The fluorescence emission spectra of Hb-FeQCs (300 μL 500 μg.mL^{-1}) were measured in a fluorimetric cell (1 cm

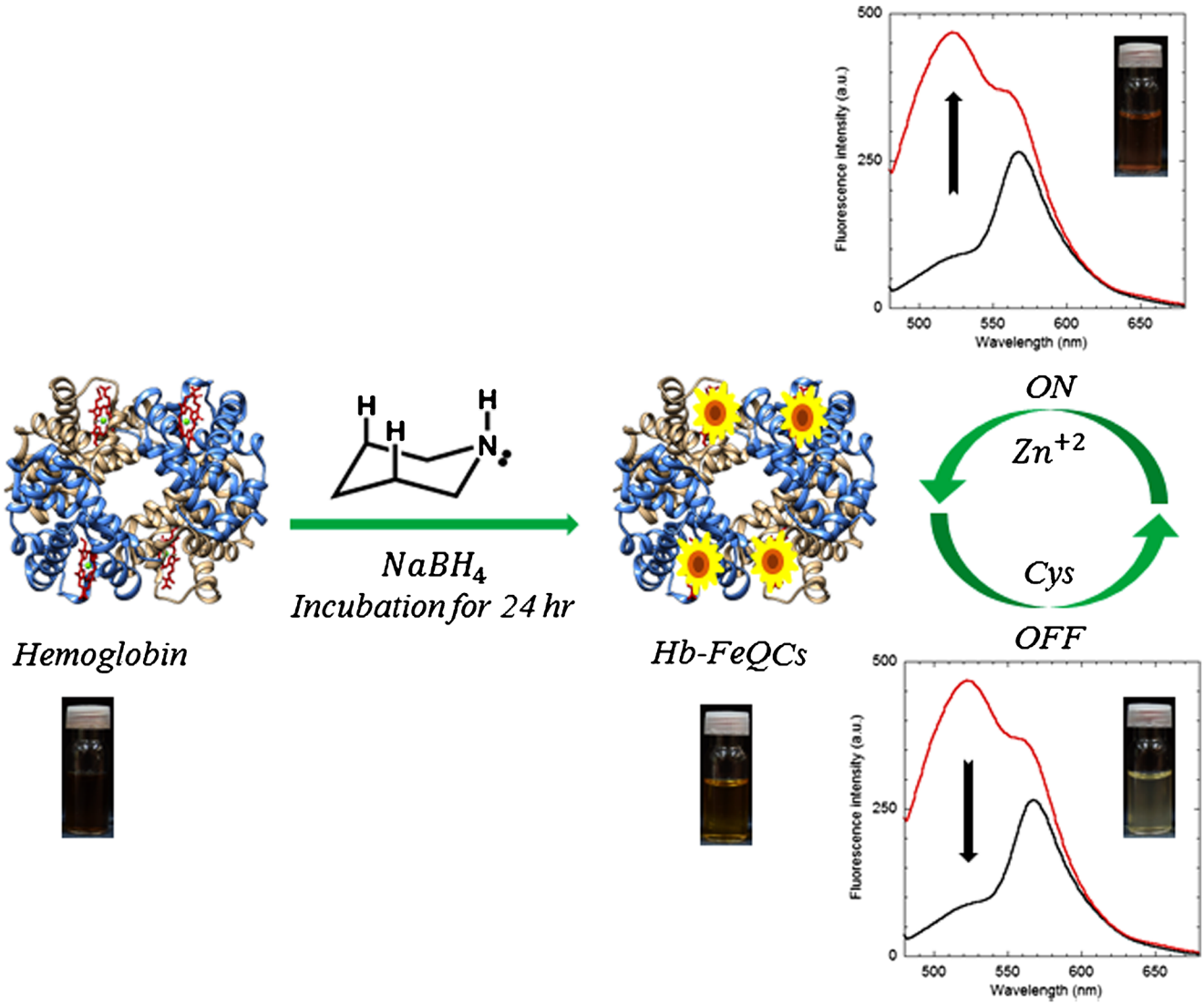

Scheme 1 Schematic presentation of the "on-off" behavior of the synthesized Hb-FeQCs probe in the presence of Zn^{2+} and Cys

path-length quartz cell) was filled with 2.2 mL solution at 25 °C, following excitation at λ: 460 nm. This solution was then titrated with standardized zinc and Cys solution (1.0 mM, final concentration: 25.0 μM) and the fluorescence intensity of the system was measured again. Spectral bandwidths of monochromators for excitation and emission were set at 10 nm. More details about experiments are in ESM.

Results and discussion

In order to extraction of iron from the porphyrin bound in the Hb-matrix, piperidine was used and followed the reduction of Fe^{2+}/Fe^{3+} with $NaBH_4$ at room temperature. After the freeze-drying, the lyophilized product was suspended in water; the solution turned yellowish brown and showed yellow luminescence under UV light. Compared to Hb with a red color (Fig. 1A), the changes are observed in the oxidation state of the Fe atom to make luminescent FeQCs. While Goswami [6] has employed strategies of ligand exchange and phase transfer of the cluster from water to chloroform for structural characterization, here for the first time the several spectroscopic methods are used to characterize the Hb-FeQCs complex system in aqueous solution. This highly luminescent protein protected cluster is being used as a sensor for monitoring Zn(II) in biological contexts; at the same time, it allows detection of Cys with tunable sensitivity and offers high selectivity for Cys over other amino acids.

Characterization of Hb-FeQCs

The prepared Hb-FeQCs were characterized using different methods. Some of these methods include FTIR spectroscopy, Circular dichroism (CD), Dynamic light scattering (DLS), Vibrating sample magnetometer (VSM), Photoluminescence, and UV–vis spectroscopy. Since FTIR technique is an

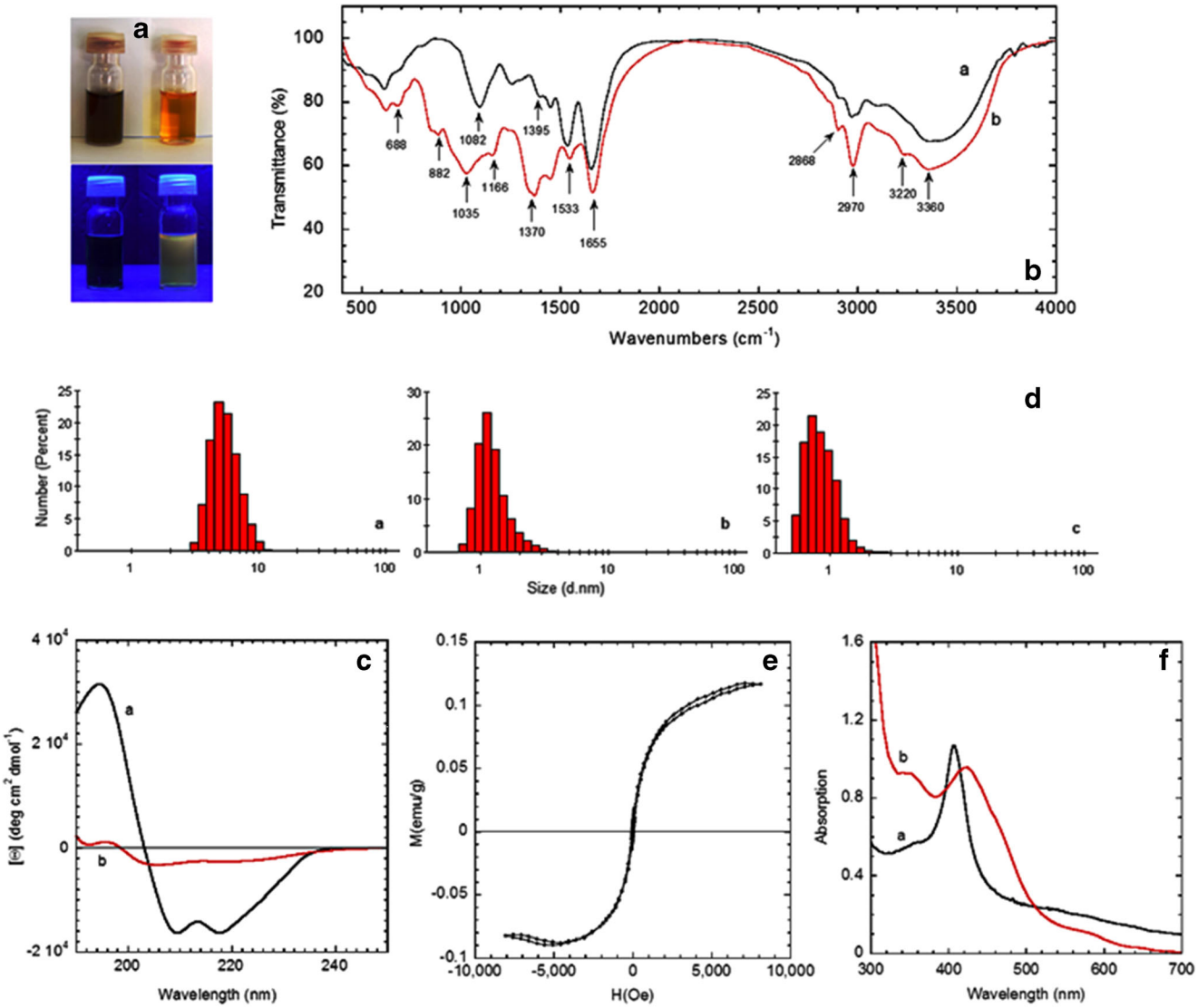

Fig. 1 (**A**) Upper panel: photographs of Hb (left) and Hb-FeQCs (right) in water piperidine solvent and lower panel: their corresponding photographs under UV light, respectively. Change in color from brown to yellow under visible light indicates the change of Fe oxidation state (**B**) FT-IR spectra of free Hb (a) and Hb after FeQCs formation (b), demonstrating changes in the secondary structure of the protein (**C**) CD spectra of free Hb (a) and Hb after FeQCs formation (b), demonstrating changes in the α-helical content of Hb following QCs synthesis (**D**) Average hydrodynamic diameter of (a) hemoglobin (b) hemoglobin/ Piperidine and (c) Hb-FeQCs determined by dynamic light scattering (**E**) Vibrating sample magnetometer data of Hb-FeQCs plotted after subtracting the diamagnetic background from the sample holder (**F**) UV–vis absorption spectra of (a) free Hb and (b) Hb-FeQCs

appropriate tool to identify the conformational sensitive binding of Hb sites with the nanoclusters, the FTIR spectra of (a) Hb and (b) Hb-FeQCs are compared in Fig. 1B (a, b). There were changes in the intensity or position of the amide I band mainly from C=O stretching (1600–1700 cm^{-1}), an amide II band assigned to N–H bending and C–N stretching (1480–1575 cm^{-1}), in comparison with the spectrum of native Hb, providing evidence for the FeQCs formation and changes in the protein structure [16]. By comparing the two spectra, we can see a decrease in the intensity of the amide I (1650 cm^{-1}) of the Hb immobilized on the Hb-FeQCs that is close to the free Hb (1655 cm^{-1}), while the amide II (1533 cm^{-1}) and the aromatic amine bands (1395 cm^{-1}) in free Hb are disappeared in Hb-FeQCs in the expense of appearance of a new band at 1370 cm^{-1}. The large decrease in the intensity of the amide I region suggests that there is a significant deformation in the conformation of the Hb from its free state to that in the Hb-FeQCs. Hb is known to bind to FeQCs via its free amine [17]. The band at 3405 cm^{-1} is related to the stretching vibration of N–H of the amide group and increase of the saturated C-H stretching modes around 2970 cm^{-1} band is evidenced the presence of piperidine [18].

Ion–protein as well as protein–nanomaterial interactions were monitored using CD spectroscopy. It can get an insight into the changes of the helical structure of Hb, therefore, the CD spectra of the protein in (a) native form and in (b) Hb-FeQCs system were recorded in far-UV region of <250 nm

(Fig. 1C a,b). It is known that when the free Hb molecule existed in α-helical structure, there are positive CD at ~193 nm and two negative CD bands at ~209 nm and ~220 nm. The 209 nm band relates to π-π* transition of the α-helix, whereas the 220 nm band belongs to π-π* transition for both the α-helix and random coil. On the other hand, a positive (190 nm) and a negative (215 nm) band are expected to appear for the existence of β-sheet [19]. The formation of Hb-FeQCs results into changes in ellipticity at 193, 209 and 220 nm and a blue shift in the band at 209 nm compared with the spectrum of native Hb. In this regard, the secondary structural elements were calculated by the J-715 Standard Analysis program and the results show that the pure Hb contains ~81% α-helix, which complies with earlier results of Hb [20]. While the Hb-FeQCs revealed a 62 and 48% decrease in α-helical and β-sheet, respectively, 25% increase in random coil structures; thus, these conformational changes indicate loss of α-helix stability and unfolding of Hb after QCs formation.

Light scattering method along with the zeta potential measurements were used to measure the hydrodynamic sizes of the particles in solution to confirm the stability of the Hb-FeQCs. As shown in Fig. 1D, compared with the size of (a) hemoglobin, (b) hemoglobin/piperidine, and (c) several tiny particles of nearly uniform size are spread over the grid with a core size of less than 1 nm, which is also confirmed by high resolution transmission electron microscopic (HRTEM) [6]. In addition, a great electrostatic repulsion between particles was achieved from the zeta potential value (−27.7 ± 7.7 mV) of Hb-FeQCs in solution. It should be noted that the measured zeta potential of Hb-FeQCs is about (17 mV) more negative than that of Hb alone (−10 ± 5.52 mV) at a pH of 7.4 confirming the formation of Hb-FeQCs [15]. Thus, the particle sizes and the zeta potential data agree with the assembly of FeQCs and the Hb protein in solution. The most appropriate method to measures the magnetic properties of a small sample of a magnetic core is vibrating sample magnetometer (VSM). As shown in Fig. 1E, the saturation moments obtained from the hysteresis loop was 12×10^{-2} emu.g^{-1} for Hb-FeQCs, while it was near 0.08 for pure Hb, which indicates the super-paramagnetic behavior of the FeQCs. In order to verify the in situ formation of FeQCs, UV–vis absorption spectroscopy was conducted. The absorption spectra of aqueous solutions of FeQCs and native Hb are shown in Fig. 1F. Compared with the spectrum of (a) pure Hb, (b) the Hb-FeQCs showed discrete bands centered at 344, 420, and 639 nm, in which molecule-like discrete bands are unique to QCs [21].

Also, the absence of any characteristic band corresponding to iron nanoparticles (FeNPs) (at 360 nm) further confirmed that the FeQCs present in the aqueous phase were mostly free of large NPs and were nearly pure in the synthesized form [22], and the photoluminescence spectra of the Hb-FeQCs were found locate in 567 nm, when excited at 460 nm with maximum emission (Fig. 2 A).

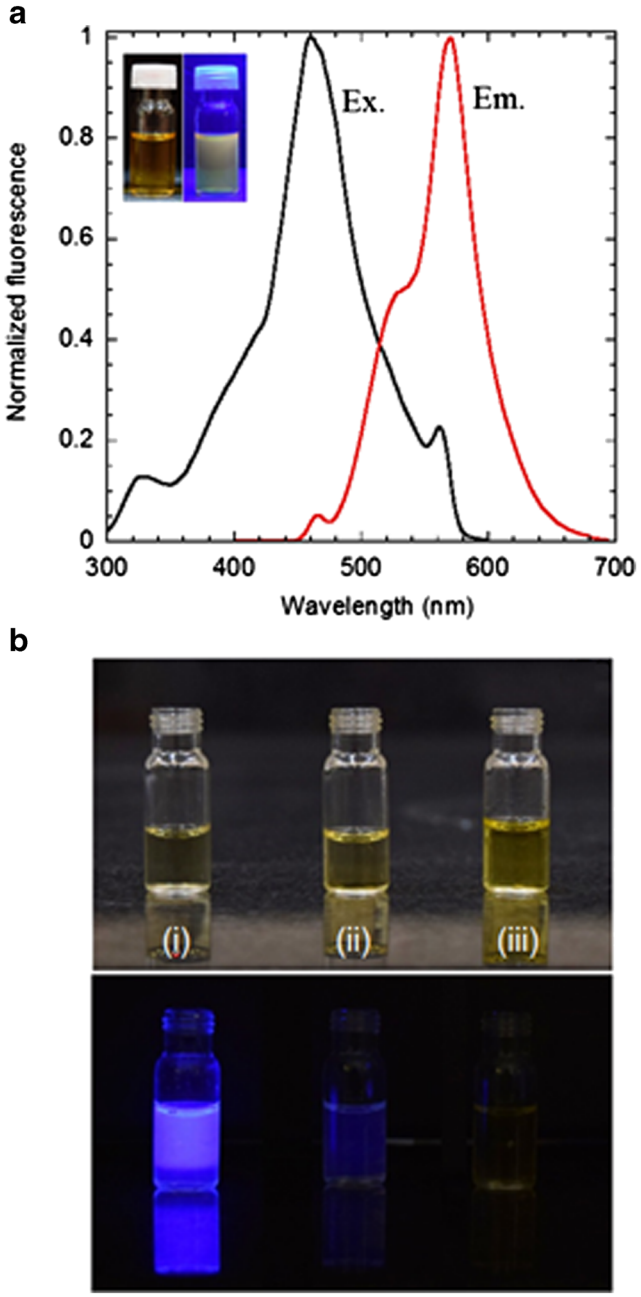

Fig. 2 (**A**) Excitation and emission spectra of Hb-FeQCs at room temperature, (black and red line, respectively), the inset contains the photographs of the Hb-FeQCs under visible and UV light. (**B**) Upper panel: bright field photographs of the mixed luminol–(i) Hb (ii) Hb/piperidine and (iii) Hb-FeQCs. Lower panel: dark field photograph of the mixtures after the injection of hydrogen peroxide. In the case of Hb-FeQCs, the solution does not show any chemiluminescence revealing that Fe is in the zero oxidation state

To verify the oxidation state of Fe in the cluster, we performed "a cold light experiment". Briefly, each *heme* group is a catalyst for the chemiluminescence reaction, this makes the luminol to extremely shiny blue in the presence of peroxide [23]. During this redox reaction, Fe^{2+}/Fe^{3+} are reduced with the concomitant oxidation of H_2O_2 to O_2. However, Fe cannot

catalyse the chemiluminescence reaction, if it will be in the 'zero' oxidation state. While the chemiluminescence observed for the Hb had very high intensity, it decreased several folds in the presence of piperidine as a reducing agent to the luminol–hydrogen peroxide mixture (Fig. 2B). In other words, the blue glow in a mixture of luminol and H_2O_2 is not produce in the present of Hb-FeQCs, suggesting that the prepared QCs are in the metallic state.

The effect of buffer solutions on the fluorescence of Hb-FeQCs at 567, 520 nm was studied over a pH range of 5–12 (Fig. S1). The results showed that the fluorescence intensity obtained at each pH value did not significant differ in buffered and unbuffered solutions but the trend of pH affects was similar. Since there were the same optimal conditions for pH 7.0, thus, aqueous medium is selected for further studies (see SEM for more detail).

Preliminary studies

The qualitative estimation of the affinity of the sensor Hb-FeQCs (500 μg.mL^{-1}) towards various metal ions is performed visually to evaluate whether analyte can be easily followed by monitoring the changes in UV–vis absorption spectra of the receptor Hb-FeQCs, (Fig. 3). With addition of zinc solution (1.0 mM), instantaneous color changes are observed from light yellow to light orange, while no detectable color changes are seen even with the addition of a large excess of other metal ions to the sensor Hb-FeQCs. However, there is an interesting colorless copper and cobalt solution. The result indicated that the color changes are most probably because of the formation of a new complex species with different electronic properties from that of the receptor Hb-FeQCs, and therefore a new color is observed.

Excellent sensitivity for Zn^{2+} is revealed from fluorescence titration of Hb-FeNCs with various metal ions and the results are explained in Fig. S2 (ESM).

Fig. 4A illustrates the absorption spectra recorded on titrating of Hb-FeQCs (500 μg.mL^{-1}) in water with a standard solution of zinc (1.0 mM). It is obvious that Hb-FeQCs is characterized by a broad absorption band which appears at 425 nm. As soon as Zn^{2+} ion was added to the Hb-FeQCs solution at room temperature, the absorption maximum of Hb-FeQCs at 425 nm gradually decreased and a new band at 520 nm increased, suggesting an intramolecular charge transfer (ICT) band in the clear isosbestic point at 460 nm [24]. Therefore isosbestic point wavelength is selected for exciting both the quantum cluster and the newly formed complex. This stable complex with a certain stoichiometric ratio has formed between Hb-FeQCs and Zn^{2+} ion in the visible region.

Signal-on fluorescence detection of Zn^{2+}

Figure 4B presents the fluorescence emission spectra with different Zn^{2+} concentrations from 0.04 μM to 25 μM to Hb-FeQCs solution. A significant increase in fluorescence occurred with the increase of Zn^{2+} concentration. The maximum emissive wavelength shifted from 567 nm to 520 nm, indicated the possibility of use of Hb-FeQCs as a highly sensitive "turn-on" fluorescence probe for Zn^{2+} ion. The high selectivity of this probe is derived from the high affinity of piperidine for Zn^{2+} [25]. From other point of view, a significant increase in fluorescence intensity is observed for Hb-FeQCs. The new peak emission (520 nm) of the complex Hb-FeQCs compared to that at 567 nm of the free Hb-FeQCs is quite unexpected (Fig. 4B). The emission of the free Hb-FeQCs would expect to be in a higher energy than that of the complex due to its relatively high-energy excitation band. The excited-states resulting from complexes of Zn^{2+} are typically ligand-centered (LC) in nature because d^{10} metal centers are not able to participate in low energy charge transfer for metal-centered transitions, leading to unexpected emission peak of the complex. On the other hand, reduction of Iron(III) porphyrin complexes in excess of amine results in the formation of hexa-coordinated Iron(II) products through stabilizing axial ligation of the metal center [26]. Several criteria must be met for metalation: porphyrin ring distortion, followed by pyrrole proton loss, then outer-sphere complexation, and iron-ligand dissociation. This porphyrin core distortion mode is also sensitive to substitution on the porphyrin ring in addition to the oxidation state of the metal. Since Zn^{2+} typically is found to assemble coordination complexes with four ligands in a tetrahedral geometry, we suggested that it is this zinc which is exchangeable for iron-piperidine complex and which causes the significant shift in fluorescence spectra [27, 28]. For taking account of all potential products that might have formed after the reaction of piperidine and

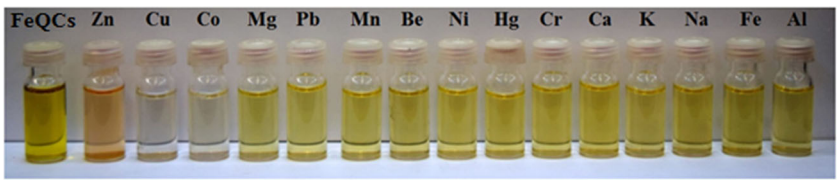

Fig. 3 Color response of the receptor Hb-FeQCs (**L**) in water (500 μg.mL^{-1}) to the addition of metal ions (1.0 mM) from the left to the right: Hb-FeQCs only, **L** + Zn^{2+}, **L** + Cu^{2+}, **L** + Co^{2+}, **L** + Mg^{2+}, **L** + Pb^{2+}, **L** + Mn^{2+}, **L** + Be^{2+}, **L** + Ni^{2+}, **L** + Hg^{2+}, **L** + Cr^{2+}, **L** + Ca^{2+},**L** + K^{+}, **L** + Na^{+}, **L** + Fe^{3+}, **L** + Al^{3+}

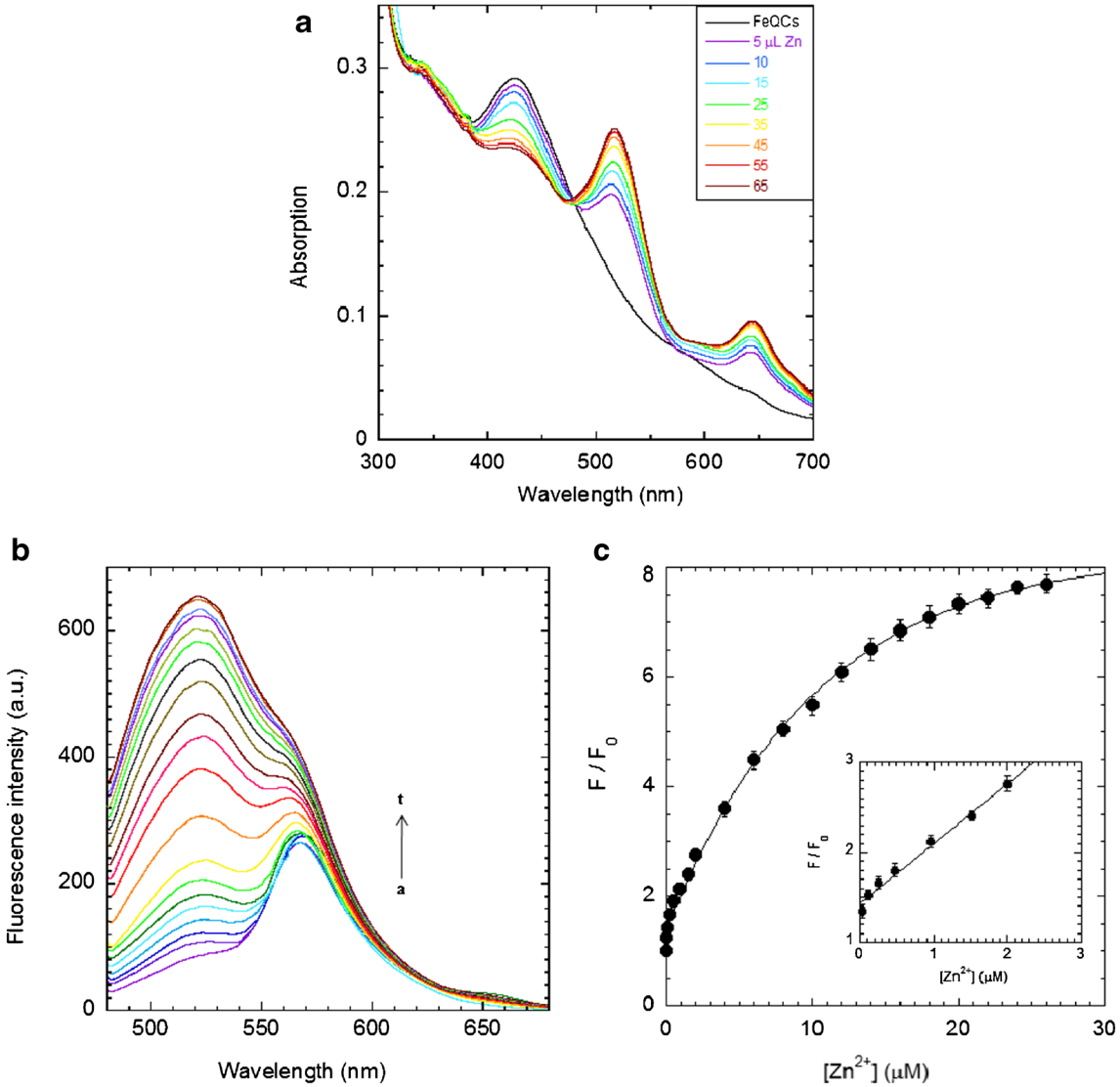

Fig. 4 (**A**) Changes in the UV–vis spectra of Hb-FeQCs (500 μg.mL^{-1}) upon addition of Zn^{2+} (1 mM) in aqueous solution (**B**) Fluorescence titration of Hb-FeQCs (500 μg mL^{-1}) in aqueous solution in the presence of varying concentrations of Zn^{2+} ion: (a) 0, (b) 0.04, (c) 0.12, (d) 0.24, (e) 0.48, (f) 0.96, (g) 1.52, (h) 2.0, (i) 4.0, (j) 6.0, (k) 8.0, (l) 10.0, (m) 12.0, (n) 14.0, (o) 16.0, (p) 18.0, (q) 20.0, (r) 22.0, (s) 24.0, (t) 26.0 μM, (λ_{ex}:460 nm). (**C**) Calibration plots of fluorescence ratio (F/F_0) of Hb-FeQCs at 520 nm versus concentrations of Zn^{2+} .Inset shows the linear range from 0.1 to 2.0 μM; error bars represent ±3σ, $y = 1.438 + 0.6655\times$, $R^2 = 0.99193$

$NaBH_4$, several control experiments was performed in the presence of specific proteins such as protoporphyrin. The results of these observations indicated that in the present of zinc the porphyrin moiety alone and globular chain of protein are not involved but iron quantum cluster is responsible for the 520 nm fluorescence peak.

The fluorescence emission intensity of Hb-FeQCs was linear as a function of Zn^{2+} concentration in the range of 0.1–2.0 μM with a regression eq. ($F/F_0 = 0.6655[Zn^{+2}] + 1.438$, $R^2 = 0.99193$) (Fig. 4C). The calculated limit of detection was as low as 48 nM ($S/N = 3$), which far lower than previous reports [29]. It was also far below the guidelines of the WHO for drinking water (76 μM) [30], and the physiological content in human serum(10 μM) [31].

Several studies about visible wavelength fluorescent Zn^{2+} probe such as Newport Green (NPG) were shown a good Zn^{2+} specificity but a relatively low affinity and a relatively small dynamic range [32], However, it is unable to image free Zn^{2+} ion in native systems because of its stability constant for Zn^{2+} is too small. Therefore, synthesized quantum clusters in solution have been indicated as a new Zn^{2+}-selective fluorescent probe with excitation wavelength under visible lamp.

Signal-off fluorescence detection of cysteine

Common Zn^{2+} ligands found within proteins include cysteine (C), histidine (H), aspartate (D), and glutamate (E) residues. The ability of cysteine to bind metals due to the ionization

state of its thiol group can display high affinity toward zinc ions, therefore Zn^{2+}-cysteine complexes are sensitive sensors. To explore the selectivity of our sensor system, tests of other 19 essential amino acids at a concentration of 150 μM were measured and the results are shown in Fig. 5. As seen, amino acids did not produce any noticeable effect on the emission of Hb-FeQCs, in the absence of Zn^{2+} ions (Fig. 5A blue), but the increased fluorescence of the Hb-FeQCs/ Zn^{2+}system was attributed to the removal of the Zn^{2+} by Cys from the surface of the Hb-FeQCs (Fig. 5A red). Here, the coordination interaction between Zn^{2+} and Sulphur atoms of Cys plays a significant role in dissociating Zn^{2+} from the surface of FeQCs [33]. Based on results, the fluorescence turn-off assay showed a highly selectivity detection for cysteine against all other essential amino acids.

The Hb-FeQCs/Zn^{2+} emission are affected from cysteine and the maximum emission peak at 520 nm linearly decreased, especially the emission is nearly completely reached to the first emission of Hb-FeQCs in the presence of 60 μM cysteine (Fig. 5B). As shown in Fig. 5C, the corresponding plot of (F_0/F) versus [Cys] indicated two excellent linear correlations graphs with correlation coefficients $R^2 = 0.9957$ and 0.9900, over the cysteine concentrations 1.0–20.0 μM (F_0/F = 0.096093 [Cys] + 1.3087) and 20.0–60.0 μM (F_0/F =

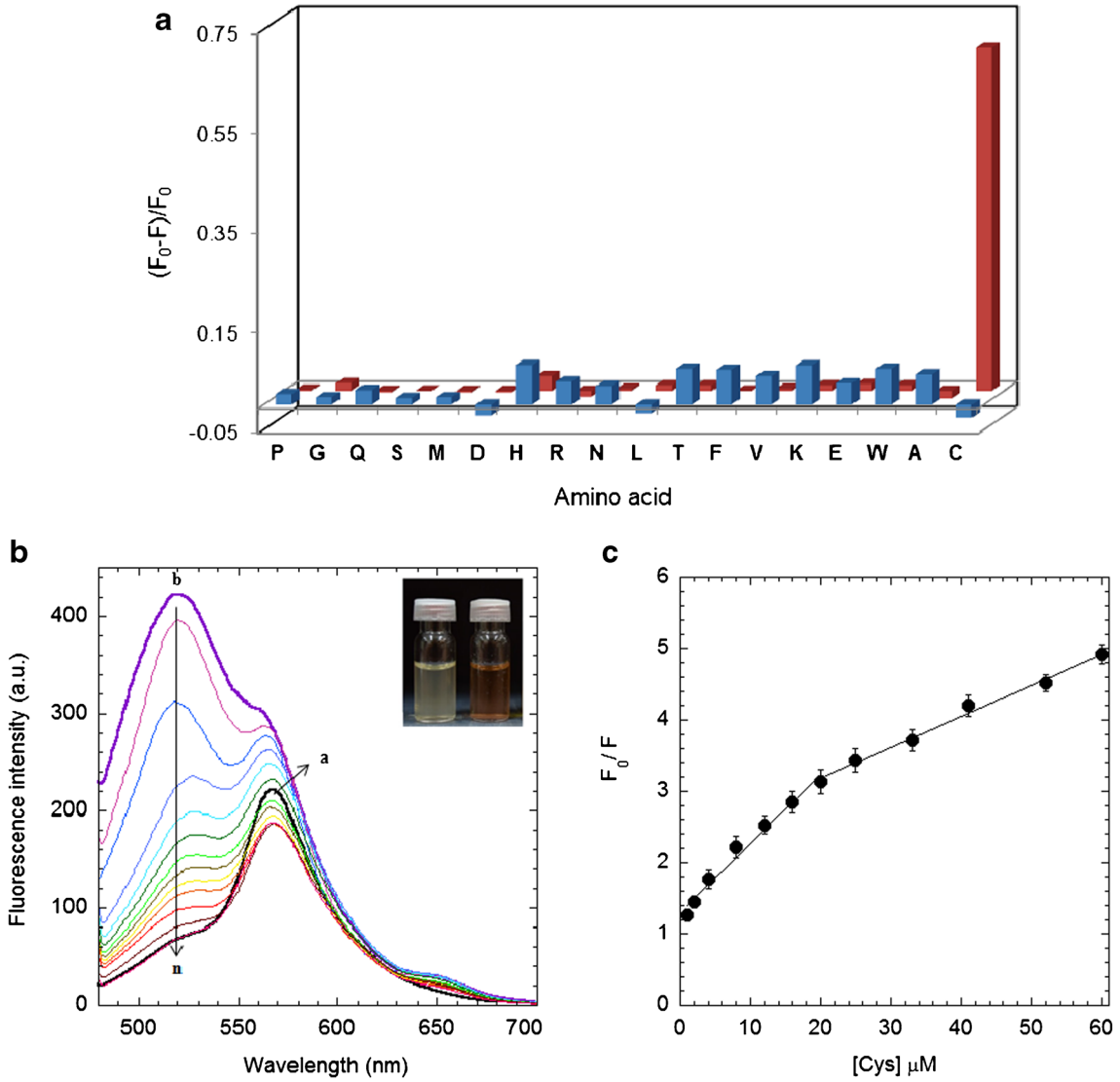

Fig. 5 (**A**) Fluorescence emission response profiles of Hb-FeQCs (500 μg mL^{-1}) in the absence (blue, front) and presence (red, back) of 20 μM Zn^{2+} ion towards 150 μM concentration of different amino acids: (P) Pro, (G) Gly (Q) Gln, (S) Ser, (M) Met, (D) Asp, (H) His, (R) Arg, (N) Asn, (L) Leu, (T) Thr, (F) Phe, (V) Val, (K) Lys, (E) Glu, (W) Trp, (A) Ala, (C) Cys. (**B**) Fluorescence spectra of Hb-FeQCs containing Zn^{2+} in the absence and presence of increasing amounts of Cys (from 0 to 60 μM) at 520 nm (λ_{ex}:460 nm): (a) 500 μg mL^{-1}HbFeQCs (b) a + 20 μM Zn^{2+}, (c) to (n) b + varying concentration of Cys: (c) 1, (d) 2, (e) 4, (f) 8, (g) 12, (h) 16, (i) 20, (j) 25, (k) 33, (l) 41, (m) 52, (n) 60 μM. The inset showed the colour progression after the Hb-FeQCs/Zn^{2+} titrated with 60 μM of cysteine (**C**) Corresponding plot of (F_0/F) versus Cys concentration at 520 nm (λ_{ex}:460 nm); error bars represent ±3σ

0.043477[Cys] + 2.3138), respectively, the sensitivity of the second calibration curve at higher Cys concentration being lower than that of the first one. The LOD was calculated to be 0.25 μM (S/*N* = 3), which is reasonable for the detection of micro molar concentrations of the Cys. This is reasonable because S in cysteine as a soft base tends to match a Zn atom of soft acid and the ability of the Zn^{2+} as a Lewis acid often limits because of occupying more ligand sites by cysteine as a strong nucleophilic agent, therefore, these complexes relatively inert [34]. We also investigate the sensitive colorimetric assay of this system for different types of S-containing chemicals such as glutathione (GSH), biotin, and bio thiols at the similar concentrations in an aqueous system. The results revealed the good sensitivity and selectivity toward cysteine of this colorimetric detection. The color of solution is changed from light pink to light green with increase of Cys concentration (the inset in Fig. 5B). Table S1 in the ESM lists the comparison of assay performance between the Hb-FeQCs and other luminescent nanoprobes for Zn^{2+} and Cys detection.

Selectivity

To evaluate the selectivity of Hb-FeQCs as a fluorescent probe for Zn^{2+} ions, the interference effects of 15 different cations, including alkali, alkali earth, transition and heavy metal ions were investigated on the response behavior of the prepared sensing system by recording the fluorescence spectra of probe in the presence of competing metal ions (Fig. 6 black histogram). As expected, Hb-FeQCs fluorescence is slightly influenced by the addition of K^+, Ca^{2+}, Na^+, Fe^{3+}, Mg^{2+}, Hg^{2+}, Be^{2+} and Al^{3+}. A fluorescence quenching with the addition of Cu^{2+} is detected, while, an enhancing fluorescence is observed for Hb-FeQCs upon binding to Zn^{2+} by comparison with that of only Hb-FeQCs in the solution.

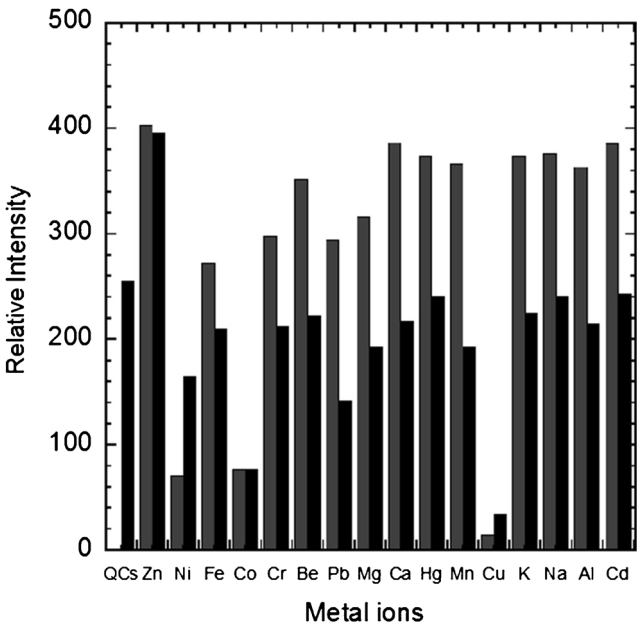

Fig. 6 Fluorescence responses of Hb-FeQCs (2.5 mL, 500 μg mL^{-1}) upon addition of cations (50 μM) (λ_{ex}: 460 nm, λ_{em}: 567 nm) (black bar) and fluorescence responses of Hb-FeQCs (2.5 mL, 500 μg mL^{-1}) containing 50 μM Zn^{2+} and the background cations (100 μM) (gray bar) (λ_{ex}: 460 nm, λ_{em}: 567 nm)

Competition experiments in the presence of Zn^{2+} and double equivalents amounts of background metal cations were performed (Fig. 6 gray histogram) and the results show that the fluorescence of Hb-FeQCs upon binding to Zn^{2+} did not significantly change in the presence of other metal ions except the transition metal Cu^{2+}, Ni^{2+} and Co^{2+} quenched the emission ratio to some extent, which it can be explained as follows. Paramagnetic ions like Cu^{2+} ion with a free d shell cause a photo-induced metal to fluorophore electron which can strongly quench the emission of a fluorophore or an energy transfer mechanism as observed in other Cu^{2+}-recognition sensors. However, Cu^{2+}, Ni^{2+}, and Co^{2+} ions present in the low concentrations have little influence on living cells. Also, when both the ions are likely to be present, selective detection of Zn^{2+} in the presence of Cd^{2+} becomes important in the environmental matrix [35]. In this regard, no obvious variation was observed in fluorescence intensity in the presence of Cd^{2+}; therefore, Hb-FeQCs has excellent selectivity for Zn^{2+} over other metal cations.

In vitro bio-imaging and cellular uptake

The response of the probe to Zn^{2+} in the cultured HFF cells was performed to demonstrate the cellular uptake of Hb-FeQCs and its potential for the detection of Zn^{2+} in the biological system. The low toxicity effect of Hb-FeQCs/Zn(II) on the viability of cells is shown in Fig. S3. In the experiments, the solution of Hb-FeQCs was added to the cells cultured in 24-well plates and incubated for 10 min then treated with Zn^{2+} for 30 min at 37 °C. Fig. 7A, D displays the bright field transmission of HFF cells which incubated with Hb-FeQCs and Zn^{2+}, respectively. The strong green-yellow fluorescence is observed after exposing to Hb-FeQCs, which demonstrated the penetration of the QCs into the cell Fig. 7B. On the other hand, the fluorescence intensity obviously increased by further incubation of the cells with Zn^{2+} (30 μM), the yellow fluorescence was much stronger and clearly observable even under visible lamp (graphical abstract). This suggests that the new complex can form inside the cell. This yellow fluorescence substantially increased upon introduction of zinc (Fig. 7E). An overlay of the fluorescence and bright-field images indicates that the fluorescence signals are located in the local intracellular area and present the subcellular distribution of Zn^{2+} with cell-membrane permeability of Hb-FeQCs (Fig. 7C, F). It can be concluded that switch detection system can detect Zn^{2+} in living HFF cells, which indicates the potential utility of the probe for Zn^{2+} detection in the biological system.

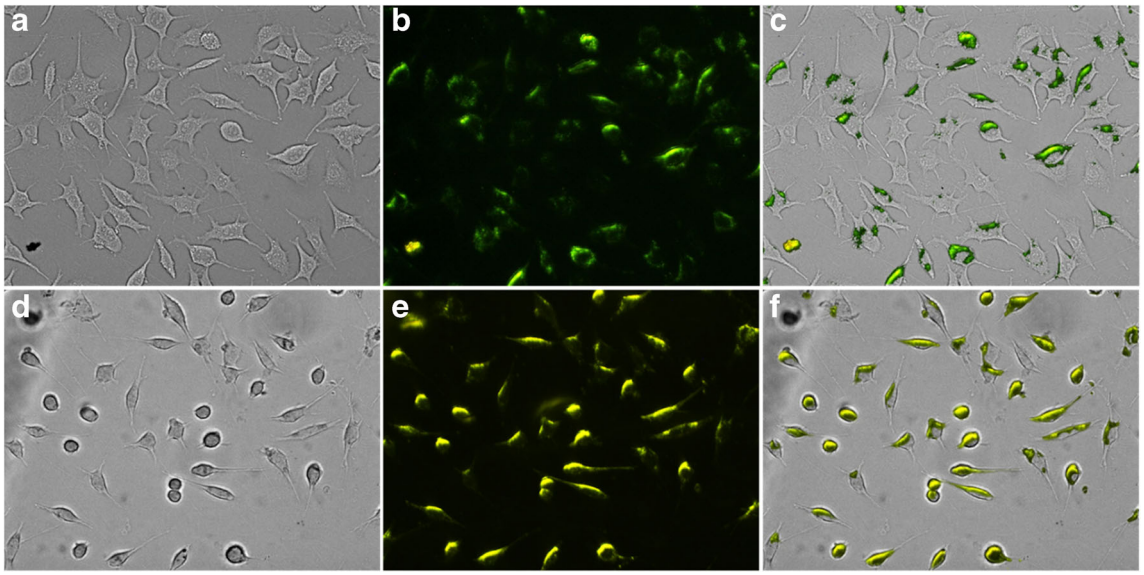

Fig. 7 Live-cell imaging of HFF cells after incubation with Hb-FeQCs (0.5 mg mL^{-1}): (**A**) Bright-field microscopy image. (**B**) Greenish-yellow fluorescence image without addition of Zn^{2+} (λ_{ex}:460 nm) (**D**) Bright-field image of cells treated with 50 μM Zn^{2+} for 30 min (**E**) Strong yellow fluorescence image of Hb-FeQCs/ Zn^{2+} and (**C**, **F**) merged images

Conclusions

In summary, we have reported the characterization of novel water-soluble iron quantum clusters in the hemoglobin matrix, as an iron-containing oxygen-transport metalloprotein in erythrocytes, which are highly luminescent, sensitive, and very low toxic for in vivo imaging and bio-sensing of metal ions and it can be eventually useful for metalloneurochemistry studies. Then we showed by a combination of colorimetric and spectrofluorometric approaches that the yellow-emitting iron quantum clusters can be used for the preparation of ratio metric turn-on fluorescent probes for Zn^{2+}. The analyses of fluorescence properties of these quantum clusters reveal that the emission intensity increases with gradual addition of Zn^{2+} in aqueous solution. The emission intensities of these compounds quench or remain unchanged when other biologically and environmentally relevant metal ions are added to the system, with the exception of Cu and Co(II), which caused a modest interference.

These novel fluorescent switching behaviors were consistent with a reaction where the incoming zinc forms a "sitting atop complex" on the porphyrin macrocycle and inserts into the distorted porphyrin and piperidine groups of Hb-FeQCs. In addition, the Hb-FeQCs/Zn^{2+} complex can be useful as a "turn off" fluorescence probe for cysteine, which competitively complex with Zn^{2+} ion.

For an appropriate sensor molecule, some biological parameters such as super-paramagnetic efficacy, cell-membrane permeability, intracellular localization, and the toxicity of the excitation light should be considered and this novel fluorescence probe was successfully applied to image the distribution of Zn(II) ions in HFF cells and subsequently assessed the cell viability, which will provide a new approach to detect Zn^{2+} in biological system by taking advantages of selectivity, high sensitivity, very low toxicity, and simplicity detection under visible lamp.

Acknowledgments This research is a part of Naimeh Hashemi's doctoral dissertation. The authors would like to kindly acknowledge all the supports and funding from the University of Tarbiat Modares and Iranian National Elites Foundation. We thank Dr. Farnoush Faridbod for helpful comments on the manuscript.

Compliance with ethical standards The author(s) declare that they have no competing interests.

References

1. Jin R (2015) Atomically precise metal nanoclusters: stable sizes and optical properties. Nano 7(5):1549–1565. https://doi.org/10.1039/c4nr05794e
2. Borghei YS, Hosseini M, Khoobi M, Ganjali MR (2017) Novel Fluorometric assay for detection of cysteine as a reducing agent and template in formation of copper nanoclusters. J Fluoresc 27(2):529–536. https://doi.org/10.1007/s10895-016-1980-3
3. Hosseini M, Ganjali MR, Vaezi Z, Faridbod F, Arabsorkhi B, Sheikhha MH (2014) Selective recognition of dysprosium(III) ions by enhanced chemiluminescence CdSe quantum dots. Spectrochim Acta A Mol Biomol Spectrosc 121:116–120. https://doi.org/10.1016/j.saa.2013.10.074
4. Song H (2015) Metal hybrid nanoparticles for catalytic organic and photochemical transformations. Acc Chem Res 48(3):491–499. https://doi.org/10.1021/ar500411s
5. Habeeb Muhammed MA, Verma PK, Pal SK, Retnakumari A, Koyakutty M, Nair S, Pradeep T (2010) Luminescent quantum clusters of gold in bulk by albumin-induced core etching of nanoparticles: metal ion sensing, metal-enhanced luminescence, and

biolabeling. Chemistry 16(33):10103–10112. https://doi.org/10.1002/chem.201000841
6. Goswami N, Baksi A, Giri A, Xavier PL, Basu G, Pradeep T, Pal SK (2014) Luminescent iron clusters in solution. Nano 6(3):1848–1854. https://doi.org/10.1039/c3nr05784d
7. Shamsipur M, Molaabasi F, Shanehsaz M, Moosavi-Movahedi A (2015) Novel blue-emitting gold nanoclusters confined in human hemoglobin, and their use as fluorescent probes for copper (II) and histidine. Microchim Acta 182:1131–1141
8. Hosseini M, Vaezi Z, Ganjali MR, Faridbod F, Abkenar SD, Alizadeh K, Salavati-Niasari M (2010) Fluorescence "turn-on" chemosensor for the selective detection of zinc ion based on Schiff-base derivative. Spectrochim Acta A Mol Biomol Spectrosc 75(3):978–982. https://doi.org/10.1016/j.saa.2009.12.016
9. Xiao Q, Liang Y, Zhu F, Lu S, Huang S (2017) Microwave-assisted one-pot synthesis of highly luminescent N-doped carbon dots for cellular imaging and multi-ion probing. Microchim Acta:1–10
10. Lopez-Alonso M, Miranda M, Castillo C, Hernandez J, Garcia-Vaquero M, Benedito JL (2007) Toxic and essential metals in liver, kidney and muscle of pigs at slaughter in Galicia, north-west Spain. Food Addit Contam 24(9):943–954. https://doi.org/10.1080/02652030701216719
11. Kim KB, Kim H, Song EJ, Kim S, Noh I, Kim C (2013) A cap-type Schiff base acting as a fluorescence sensor for zinc(II) and a colorimetric sensor for iron(II), copper(II), and zinc(II) in aqueous media. Dalton Trans 42(47):16569–16577. https://doi.org/10.1039/c3dt51916c
12. Watt NT, Hooper NM (2003) The prion protein and neuronal zinc homeostasis. Trends Biochem Sci 28(8):406–410. https://doi.org/10.1016/S0968-0004(03)00166-X
13. Wu L, Guo QS, Liu YQ, Sun QJ (2015) Fluorescence resonance energy transfer-based ratiometric fluorescent probe for detection of Zn(2+) using a dual-emission silica-coated quantum dots mixture. Anal Chem 87(10):5318–5323. https://doi.org/10.1021/acs.analchem.5b00514
14. Yang M, Kong W, Li H, Liu J, Huang H, Liu Y, Kang Z (2015) Fluorescent carbon dots for sensitive determination and intracellular imaging of zinc (II) ion. Microchim Acta 182
15. Du P, Lippard SJ (2010) A highly selective turn-on colorimetric, red fluorescent sensor for detecting mobile zinc in living cells. Inorg Chem 49(23):10753–10755. https://doi.org/10.1021/ic101569a
16. Shao Q, Wu P, Gu P, Xu X, Zhang H, Cai C (2011) Electrochemical and spectroscopic studies on the conformational structure of hemoglobin assembled on gold nanoparticles. J Phys Chem B 115(26):8627–8637. https://doi.org/10.1021/jp203344u
17. Shen XC, Liou XY, Ye LP, Liang H, Wang ZY (2007) Spectroscopic studies on the interaction between human hemoglobin and CdS quantum dots. J Colloid Interface Sci 311(2):400–406. https://doi.org/10.1016/j.jcis.2007.03.006
18. Kucheryavy P, Lahanas N, Velasco E, Sun CJ, Lockard JV (2016) Probing framework-restricted metal axial ligation and spin state patterns in a post-synthetically reduced iron-porphyrin-based metal-organic framework. J Phys Chem Lett 7(7):1109–1115. https://doi.org/10.1021/acs.jpclett.6b00302
19. Mahato M, Pal P, Tah B, Ghosh M, Talapatra GB (2011) Study of silver nanoparticle-hemoglobin interaction and composite formation. Colloids Surf B Biointerfaces 88(1):141–149. https://doi.org/10.1016/j.colsurfb.2011.06.024
20. Dong A, Huang P, Caughey WS (1990) Protein secondary structures in water from second-derivative amide I infrared spectra. Biochemistry 29(13):3303–3308
21. Qian H, Zhu M, Wu Z, Jin R (2012) Quantum sized gold nanoclusters with atomic precision. Acc Chem Res 45(9):1470–1479. https://doi.org/10.1021/ar200331z
22. Guo L, Huang Q, Li X-y, Yang S (2001) Iron nanoparticles: synthesis and applications in surface enhanced Raman scattering and electrocatalysis. Phys Chem Chem Phys 3(9):1661–1665
23. Barni F, Lewis SW, Berti A, Miskelly GM, Lago G (2007) Forensic application of the luminol reaction as a presumptive test for latent blood detection. Talanta 72(3):896–913. https://doi.org/10.1016/j.talanta.2006.12.045
24. Shao J, Lin H, Lin HK (2008) A simple and efficient colorimetric anion receptor for H_2PO^{4-}. Spectrochim Acta A Mol Biomol Spectrosc 70(3):682–685. https://doi.org/10.1016/j.saa.2007.08.018
25. Dai Z, Xu X, Canary JW (2002) Stereochemical control of Zn(II)/cu(II) selectivity in piperidine tripod ligands. Chem Commun (Camb) 13:1414–1415
26. Castro C, Jamin M, Yokoyama W, Wade R (1986) Ligation and reduction of iron (III) porphyrins by amines. A model for cytochrome P-450 monoamine oxidase. Journal of the American Chemical Society 108 (14):4179–4187
27. Franco R, Moura JJ, Moura I, Lloyd SG, Huynh BH, Forbes WS, Ferreira GC (1995) Characterization of the iron-binding site in mammalian ferrochelatase by kinetic and Mossbauer methods. J Biol Chem 270(44):26352–26357
28. Papkovsky DB, Ponomarev GV, Wolfbeis OS (1996) Longwave luminescent porphyrin probes. Spectrochim Acta A Mol Biomol Spectrosc 52(12):1629–1638
29. Wang H, Sun C-L, Yue Y-H, Yin F-F, Jiang J-Q, H-R W, Zhang H-L (2013) New molecular probe for the selective detection of zinc ion. Analyst 138(19):5576–5579
30. Cohen JM, Kamphake L, Harris E, Woodward RL (1960) Taste threshold concentrations of metals in drinking water. Journal (American Water Works Association) 52(5):660–670
31. Maret W (2001) Zinc biochemistry, physiology, and homeostasis–recent insights and current trends. Biometals 14(3):187–190
32. Gee KR, Zhou ZL, Ton-That D, Sensi SL, Weiss JH (2002) Measuring zinc in living cells. A new generation of sensitive and selective fluorescent probes. Cell Calcium 31(5):245–251. https://doi.org/10.1016/S0143-4160(02)00053-2
33. Huang Z, Pu F, Lin Y, Ren J, Qu X (2011) Modulating DNA-templated silver nanoclusters for fluorescence turn-on detection of thiol compounds. Chem Commun 47(12):3487–3489
34. Lee YM, Lim C (2008) Physical basis of structural and catalytic Zn-binding sites in proteins. J Mol Biol 379(3):545–553. https://doi.org/10.1016/j.jmb.2008.04.004
35. Galceran J, Huidobro C, Companys E, Alberti G (2007) AGNES: a technique for determining the concentration of free metal ions. The case of Zn(II) in coastal Mediterranean seawater. Talanta 71(4):1795–1803. https://doi.org/10.1016/j.talanta.2006.08.027